

Continuous Local Symmetry: Connection to Reactivity and Recognition

Duc Anh Lai and Devin A. Matthews^{a)}

*Department of Chemistry, Southern Methodist University, Dallas, TX 75275,
USA*

Symmetry is one of the most beautiful yet mysterious concepts in science. In chemical systems, presence of local symmetries at specific fragments often serve as driving forces behind many physicochemical properties, including stability, spectroscopy, and reactivity. Moreover, degree of symmetry varies continuously with molecular dynamics and intermolecular interactions, making it a hidden but decisive factor. In this study, we propose a theoretical framework to quantify continuous degrees of symmetry and chirality localized within constrained regions of a molecular environment. Application of this method to reaction sites of dendralene molecules reveals strong correlations between local symmetry and molecular stability, parity-dependent behavior, and Diels-Alder reactivity. Additionally, representations of local chirality fields in porphyrins uncover unique signatures accounting for the chirality recognition power. Overall, these findings highlight the potentials of local symmetries within a molecular framework on predicting chemical properties.

^{a)}Electronic mail: damatthews@smu.edu

I. INTRODUCTION

Since the dawn of chemistry and physics, symmetry has served as both a conceptual property and a computational tool, as represented in a wide range of fundamental discoveries. In chemistry, the symmetry of nuclear and electronic distributions forms the foundation for numerous theories, such as valence shell electron pair repulsion (VSEPR) theory, frontier molecular orbital (FMO) theory, selection rules in spectroscopy, quantum degeneracy, and computational methods for structure and potential energy surface prediction. In practice, group theory and symmetry analysis provides an excellent explanation for many chemical behaviors in spectroscopy, chemical reactions,^{1,2} catalysis,³ chemical reactions,^{4,5} molecular recognition,⁶ self-assembly,^{7,8} and many others. Despite the importance of symmetry in chemical contexts, traditional analysis only characterizes molecular symmetry as an absolute property, i.e. whether a molecule possesses a certain symmetry element or not. Beyond the static equilibrium picture, the symmetry of molecular systems can also be considered from a dynamic or trajectory viewpoint. For example, rotational isomerism along the C–C σ bond in ethane causes a continuous change from D_{3d} to D_{3h} symmetry. Also, small distortions due to Jahn-Teller effects, thermal dynamics, solvent fluctuation, or crystal packing often deform ideally high symmetry, or inversely, thermally surmountable barriers can yield average structures with higher symmetry. As a result, many dynamic molecules are best understood as time-averaged symmetric ensembles. Spontaneous distortions taking place in organometallic complexes, piezoelectric materials, and crystallographic systems introduce symmetry variations and modify optical, electric, and magnetic properties.^{9–11} Organic chemistry is perhaps the area that most utilizes symmetry analysis of molecular systems. In pericyclic reactions, Woodward and Hoffmann’s rules state that the symmetry of interacting molecular orbitals must be constantly conserved for the reaction to proceed under thermal conditions, otherwise photoexcitation is necessary.¹ Moreover, biological macromolecules appear to exhibit cyclic (C_n), dihedral (D_n), and cubic (I, O, T) symmetries, governing a wide variety of functions.¹² However, their conformations may undergo drastic changes upon the binding of modulators.¹³ Therefore, a concept of continuous molecular symmetry is essential and advantageous.

The first attempt to quantify continuous symmetry realization in chemistry originated from Guye’s asymmetry product which empirically correlated with the optical activity.¹⁴

Subsequently, a number of symmetry measures based on molecular geometry,¹⁵ volume overlap,¹⁶ molecular surface topology,¹⁷ wavefunction and electron density,^{18,19} were introduced. Numerous studies have successfully applied these approaches to rationalize experimental observation.^{20,21} Since electron configuration dictates properties of a molecule, electronic density- or wavefunction-based methods are perhaps more suitable than structural and topological methods when one focuses on chemical behaviors and transformations. Particularly, electronic properties of chemical substituents may have significant impact on a local scaffold in resonance structures and charge transfer systems. Especially, when a molecule is influenced by surrounding molecules, or external perturbations, such as electric and magnetic fields, the electron density may not coincide with nuclear configuration. Moreover, a phase transition may occur in ultrafast dynamics, e.g. femtosecond to attosecond timescale, without a reorganization in nuclear positions, resulting in a spontaneous electronic symmetry breaking. It is also suggested that geometry alone may not suffice, other aspects, such as electronic effects, must also be considered when evaluating chirality,²² and correlating with functional predictions.²³ Among the aforementioned measures, Grimme’s method is the current choice for calculating global symmetry from molecular electronic structure calculations.²¹

In the modern context, and particularly as chemical structures of interest grow more complex with new experimental and computational techniques, the use of symmetry considerations for the entire molecule is restricted as perfect, global symmetry elements are no longer available for large and flexible systems. This leads to the adage, heard at times by the authors, that “all interesting molecules are C_1 .” However, in many situations a non-symmetric molecule may possess local segments that are fully or nearly symmetric, and these local symmetries can play a dominant role in representation of molecular properties such as spectroscopic shifts, bond strength, stability and reactivity. In particular, qualitative assessments of local symmetry are usually invoked to identify equivalent atoms, which determines distinct chemical shifts in molecular spectra. Additionally, even non-symmetric molecules can inherit the highest symmetry from its symmetrical substructures, e.g., propylene can be reduced to C_s semi-symmetry if one considers a chemical process that solely involves the π orbitals. Furthermore, global and local symmetry are likely dissimilar in transition metal systems due to bulky ligands. According to ligand field theory, orbital splitting in such molecules is more dependent on microscopic environment around the central metal than on

the global symmetry group of the entire complex. In many cases, coordination complexes take over pseudo-symmetry of the local symmetry at the metal site. On the other hand, defects in solid-state materials break down local symmetry and profoundly alter electrical conductivity, optical activity, hardness and ductility, ferromagnetism, catalytic selectivity and activity.

The idea of local symmetry in chemistry was first discussed in the perspective of Mislow and Siegel, connecting the local symmetry of segmented fragments to the context of molecular environment.²⁴ The authors proceed from the viewpoint that local symmetry generally exists at any point within the molecular framework, regardless if such point is an atomic center or not. From that starting point, they then develop the concept of the “chirotopicity field” as a local analogue of chirality, which exists even in overall achiral molecules. Combining this viewpoint with the concept of continuous symmetry, this notion implies that local symmetry should vary smoothly throughout the molecular environment, forming a continuous field that covers the entire molecule and its surroundings. Currently, there are few published techniques to calculate the local symmetry. One approach is to partition the molecular structure into fragments.²⁵ The main disadvantage of this method is that structural and electronic effects from the surrounding moieties are ignored. With a similar idea, Avnir and co-workers divided coordinate complexes into spherical shells, and compute the perturbative effects of outer shells on the degree of local chirality at the center metallic atom.²⁶ However, the method is largely biased by the choice of reference structure. As a consequent, the results are less selective when comparing across different systems. Grimme¹⁸ suggested that his method of computing continuous symmetry could also be partitioned into contributions from localized occupied orbitals. However, this approach does not address symmetry at arbitrary points and is inherently tied to the local topology of the orbitals.

In this manuscript, we propose a novel method to quantify the continuous local symmetry of a chemical system from the total electronic density. We first demonstrate how local symmetry correlates with chemical stability and reactivity of asymmetric diene units in dendralenes. Subsequently, we study the extent of local chirality of substituted porphyrins, and how that the local chiral information presents key signatures for the chiral recognition strength of porphyrins toward chiral carboxylic acids. These preliminary applications suggest a deep connection between continuous local symmetry and observable molecular

properties.

II. THEORETICAL METHODS

In this work, the degree of local symmetry with respect to a symmetry element R is calculated as,

$$S(R) = 1 - \frac{\|D_R - D_0\|_F}{\|D_R\|_F + \|D_0\|_F} \quad (1)$$

where D_0 is the molecular relaxed one-electron density matrix (1RDM) projected onto a local basis centered at a chosen point in space. The image density D_R is then obtained by transforming D_0 according to the matrix representation of the symmetry operation. The subscript F denotes the Frobenius norm. This measure provides a value between zero (no symmetry, i.e. the original and image densities do not overlap) to one (exact symmetry). The local basis is chosen as a set of uncontracted Gaussian functions spanning a range of angular momentum ($0 \leq l \leq 4$ in this work) and with consistent average radial extent (2 a.u. here). This choice provides sufficient angular resolution of electron density relevant to common symmetry operations and an unbiased (isotropic and radially consistent) sampling of the local environment. Additionally, by leveraging the electronic density directly, densities from any ab initio or semi-empirical computational method may be employed, as well as densities tabulated in real space.

While pre-chosen symmetry elements may be used in the computation of the symmetry measure, more commonly the parameters defining the element (e.g. axis of rotation or normal vector of a reflection) may be optimized such that $S(R)$ is maximized, although it is required that the symmetry axis pass through the chosen projection point. In many cases, the optimization surface of the symmetry axis Euler angles permits multiple local minima—a feature which merits further investigation in combination with the corresponding local axis frames.

As chirality emerges when a molecule lacks second-order mirror symmetry, we can compute local chirality (chirotopicity) by exhaustively finding optimal improper rotations for the local structure. Thus, local chirality can be obtained from the maximum value of local symmetry with respect to either reflection ($\sigma = S_1$), inversion ($i = S_2$) or higher improper rotation (S_3, \dots) as,

$$C = 1 - \max\{S(\sigma), S(i), S(S_3), \dots\} \quad (2)$$

where each of the symmetry measures is optimized with respect to the orientation of the symmetry element. Obviously, when there exists an ideal improper rotation, $C = 0$. On the other hand, any imperfect symmetry gives rise to a non-trivial value of C . At the upper limit $C = 1$, the second-order mirror symmetry vanishes and the molecule (or molecular region) is “maximally chiral”. In principle, one has to find all possible improper rotation symmetries, but high S_n axes are extremely sparse in real, stable molecules. Therefore, $S(\sigma)$, $S(i)$, and $S(S_n)$ (up to $n = 8$) are considered in chirality measures.

The density projection requires computation of the overlap matrix between SCF and local projection bases, which is performed by a custom Python code which leverages PySCF.^{27,28} All of the SCF calculations in this study are carried out in the ORCA 6.1 suite.²⁹

III. RESULTS

A. Local symmetry: A predictor of dendralene reactivity and stability

As noted earlier, the local symmetry of a molecule may diverge significantly from its global symmetry. This distinction is particularly critical because most chemical processes occur locally at specific functional sites within a molecule. Therefore, understanding local symmetry deviations is important, yet underexplored, for predicting reactivity, selectivity, and other chemical properties. In this context, the family of dendralenes stands out as an illustrative example: these molecules possess regional symmetries that are not immediately apparent from their entire structure, making them ideal systems for investigating how local symmetry variations influence chemical functionalization patterns.

Dendralenes are a class of branched, acyclic oligo-olefinic hydrocarbons, together with linear polyenes, annulenes, and radialenes. Although the unbranched systems, e.g., linear polyenes and annulenes, have been comprehensively studied since the 1970s, the two branched classes, including $[n]$ dendralenes, have just received significant attention recently.³⁰ Thanks to the groundbreaking studies of Hopf, Fallis, and Sherburn, to name a few, [3–12]dendralenes and their substituted derivatives have been successfully synthesized and investigated in terms of chemical stability, Diels–Alder (DA) reactivity, and spectroscopic properties.^{31–35} It is evident that dendralenes are beneficial molecules in organic synthesis, such as step-economic target synthesis on account of their ability to participate in diene-

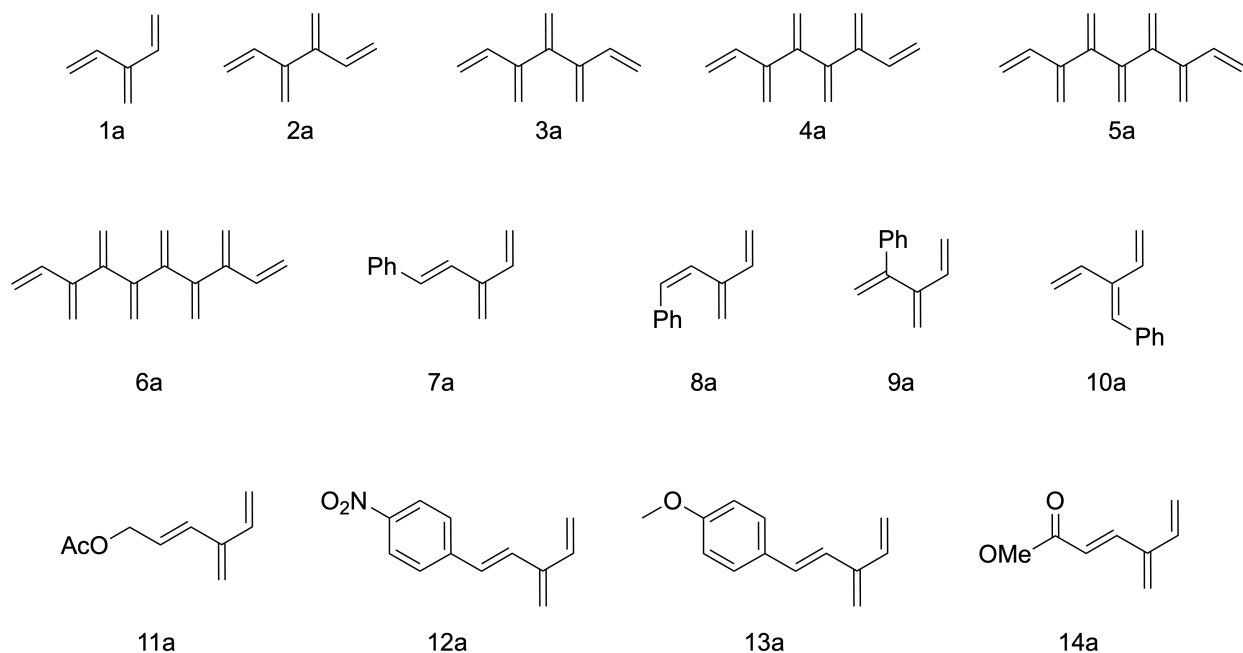


FIG. 1. [3–8]Dendralenes and derivatives.

transmissive Diels–Alder reactions.^{36,37}

A single diene, e.g. 1,3-butadiene, can adopt *s-cis*, *s-trans*, and gauche conformations depending on the dihedral angle around the internal σ bond. Since $[n]$ dendralenes possess $n - 1$ diene units arranged in a branched configuration, sp^2 carbons are twisted to sp^3 -like hybridization, mostly due to the steric hindrance of inner hydrogens. As a consequence, the torsion angles in $[n]$ dendralenes are varied largely, featuring several abnormal physicochemical properties. Efforts were made to analyze [3–8]dendralenes’ conformers, indicating that imperfect symmetries of odd and even dendralenes represent the parity-dependent behavior, the so-called alternation feature, represented in UV-Vis, ^1H and ^{13}C NMR spectra, and mono-cycloaddition DA reactivity.³⁵ The alternation behaviors are genuinely results of local diene unit properties. For example, from [4]dendralene to [12]dendralene exhibit a maximum UV-visible absorption at approximately the peak of 1,3-butadiene, suggesting that the conjugation of these systems is restricted to locally single diene structures.³⁸ It is also clear that the *s-cis* diene units, which are necessary for cycloadditions, are no longer coplanar, leading to unpredicted reactivity in the DA pathway.³⁵ In this respect, breaking of the perfect C_{2v} symmetry from an ideal *s-cis* diene may regulate the cycloaddition reaction of the dendralenes. We hypothesize that the partial symmetry descent in local quasi-*s-cis*

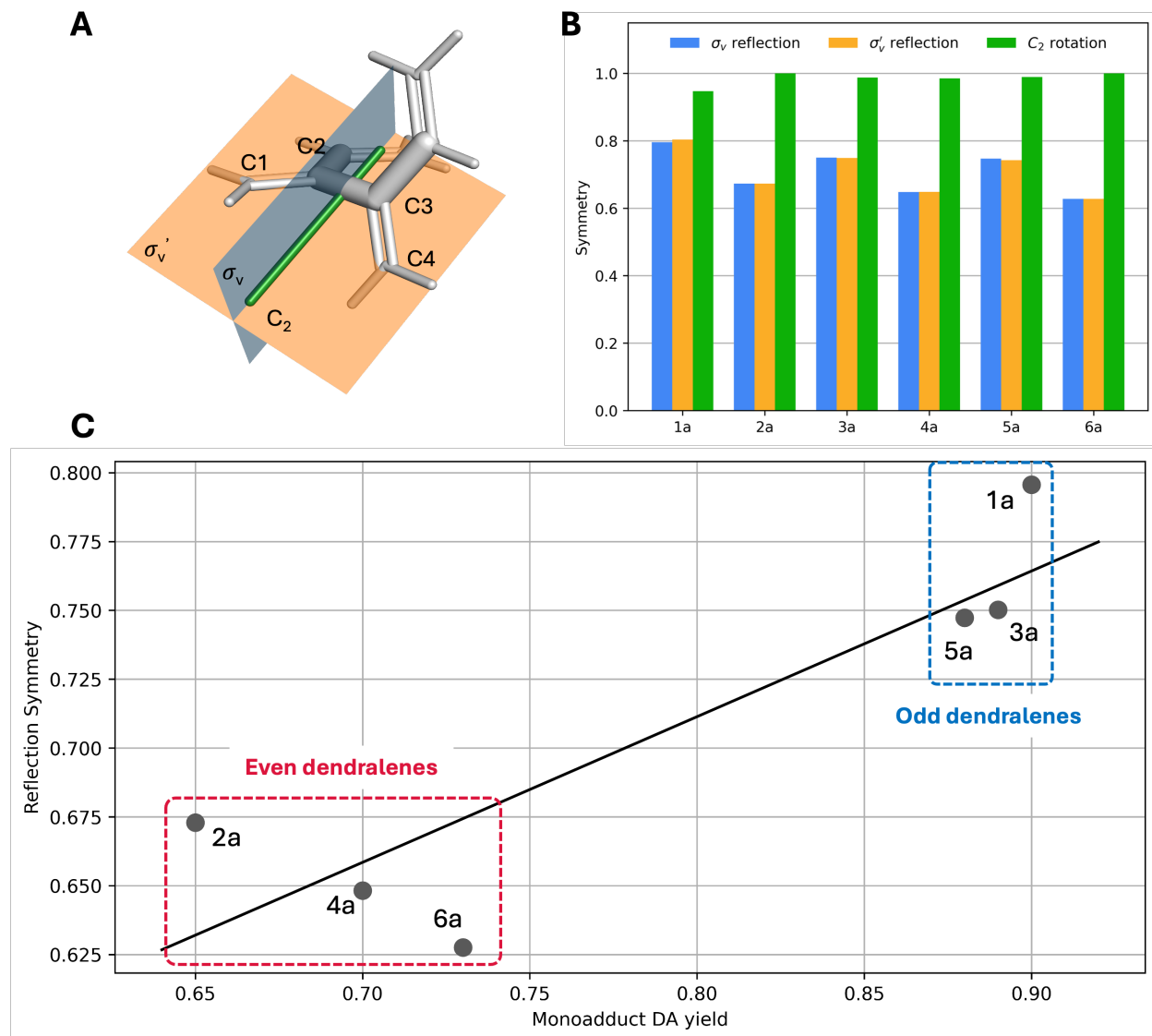


FIG. 2. **a)** Local quasi- C_{2v} symmetry elements in [4]dendralene. **b)** Local symmetry measures of [3–8]dendralenes. **c)** Correlation of local reflection symmetry (σ_v) with monoadduct Diels–Alder reactivity. Linear regression (solid line) yields a coefficient of determination of $R^2 = 0.77$.

dienes is associated with the alternation behavior of the $[n]$ dendralenes.

We performed a local symmetry analysis on quasi-cis dienes in [3–8]dendralenes (**1–6a** in Figure 1) with respect to C_{2v} symmetry. The most stable conformer of each molecule was retrieved from Saglam’s work.³⁵ First, we re-optimized molecular geometries using DFT/B3LYP/6-31G(d) with D3 dispersion correction and chloroform SMD solvation model.³⁹ Local C_{2v} symmetry of a C1-C2-C3-C4 diene consists of 3 non-trivial symmetry elements: a two-fold rotation (C_2) and two vertical reflection planes (σ_v and σ'_v) as depicted

in Figure 2a. The C_2 axis was defined by a vector connecting the centers of the C1-C4 and C2-C3 vectors. The σ_v plane bisects the diene fragment with its normal parallel to the C1-C4 vector. The other mirror plane, σ'_v , was determined such that its normal was obtained from the cross product of the σ_v normal and the C_2 axis. By construction, the two reflection planes are mutually perpendicular and both contain the rotation axis. All local symmetry computations were evaluated with at the midpoint of the C1-C4 distance.

As shown in Figure 2b, local symmetry measures clearly show the alternation feature between even and odd members of the dendralene series. We found that the symmetry measures for the two reflection planes are nearly equivalent, while local dienes exhibit an almost perfect C_2 symmetry. Therefore, the *s-cis* C_{2v} symmetry is deformed to a quasi C_2 symmetry in twisted dienes primarily by torsion of the C1-C2 and C3-C4 bonds. The lowest value of $S(C_2)$ is 0.95 in [3]dendralene, and full C_2 symmetry appears in local dienes of [4]dendralene and [8]dendralene. The [4] and [8]dendralene conformers also adopt C_2 point group for the total symmetry, showing that a connection still exists between some local symmetries and the global point group. However, as discussed below, it is the reflection and not rotation symmetry which determines local reactivity. While not required by the molecular point group, the two reflection symmetries in [4] and [8]dendralenes show no difference in magnitude. In contrast, among [3] and [5–7]dendralenes, the lower $S(C_2)$ measure corresponds to a (slightly) larger difference between the two mirror symmetry measures. This is reasonable as deviations from C_2 indicate additional perturbations which necessarily affect the C1-C2 and C3-C4 local geometries and electronic structures differentially.

More importantly, a strong correlation was observed between local mirror symmetry characteristics and mono-addict DA reactivity. In a concerted DA pathway, two new σ bonds are formed synchronously at the termini of the diene. As this process is governed by constructive orbital overlap between the HOMO of the diene and the LUMO of the dienophile (or vice versa), orbital symmetry considerations play a decisive role, and the planar *s-cis* conformation of the diene is preferred. The gauche-like functional site in dendralenes, however, make their DA reaction outcomes difficult to generalize. Experimental studies showed that odd dendralenes have substantially higher reactivity toward cycloaddition pathways than their even neighbors. This observation can be rationalized in terms of the local symmetry of the bisector plane σ_v in the local diene fragment. The highly reactive odd dendralenes exhibit significantly higher reflection symmetries compared to the nonreactive even den-

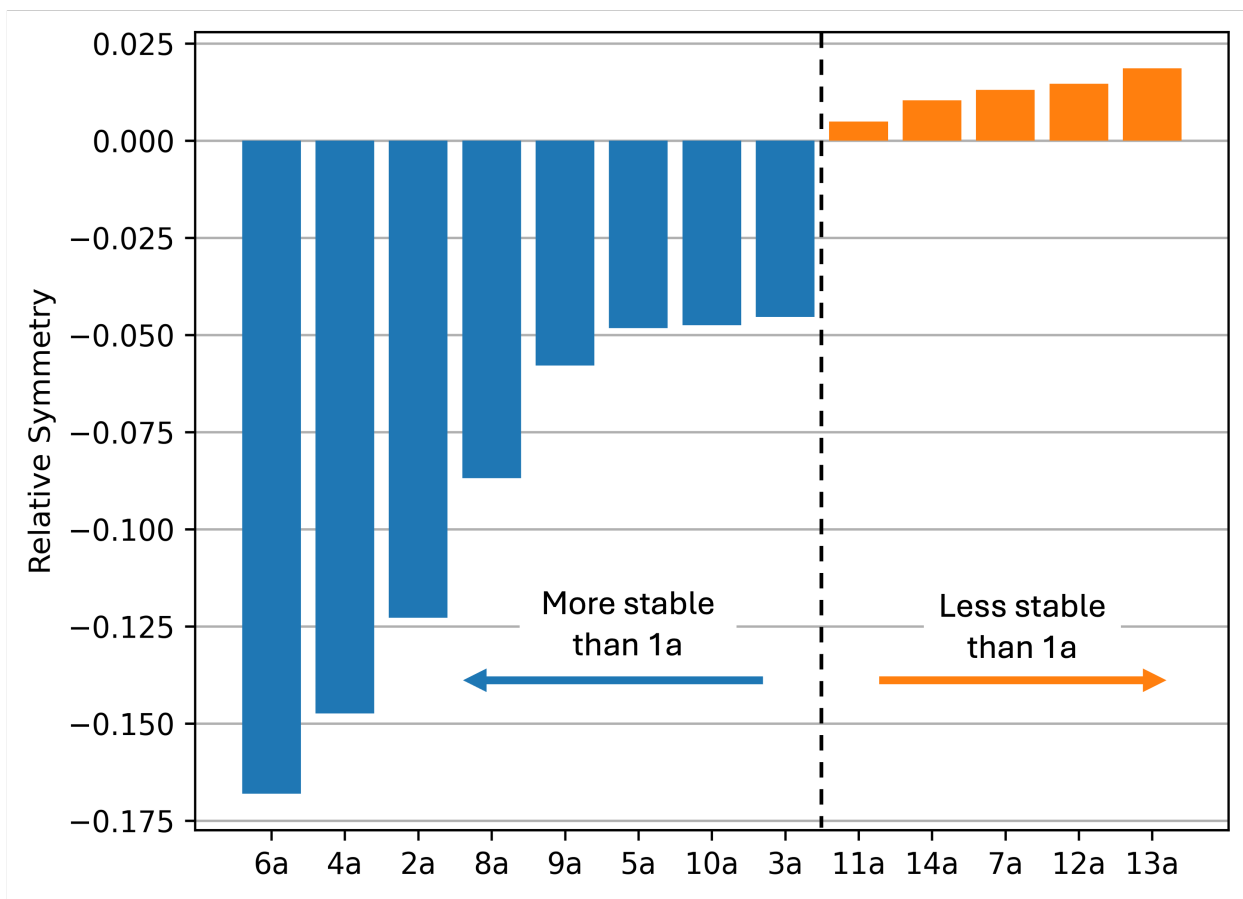


FIG. 3. Difference in local reflection symmetry (σ_v) of substituted dendralenes with respect to [3]dendralene (**1a**). Dendralenes with lower reflection symmetry are more stable than **1a** (blue), while those with higher reflection symmetry are more stable (orange). Note that species are arranged in order of local symmetry.

dralenes (Figure 2c). Linear least-squares regression yields a Pearson coefficient of 0.88, and an R^2 value of 0.77, suggesting a concrete positive relationship. The slope is statistically significant ($p = 0.021$), despite the limited sample size ($n = 6$).

The symmetry distortion of local diene groups in unsubstituted dendralenes is mostly due to the conformational steric effect of cross-conjugation. Subsequently, we included other derivatives into our test set to see whether the proposed local symmetry analysis captures electronic perturbations from chemical substituents to dendralenes in addition to purely steric effects. The substitutions vary in type of functional groups and position of modification (**7–14a** in Figure 1). Our next analysis focuses on the stability of these dendralene derivatives. The DA dimerization mechanism is proposed to explain dendralenes' stability in

pure solution. In this regards, two dendralene molecules can react with each other through a closed-shell singlet bis-pericyclic transition state. Since the essence of this mechanism is associated to the DA mechanism, it turns out that the plane of symmetry can also classify the stability of dendralenes. As shown in Figure 3, all molecules that are more stable than [3]dendralene (**1a**) have lower mirror symmetry values. The even dendralenes reported to be least reactive among dendralene family, displaying negligible decomposition over four weeks at ambient temperature, present the highest degree of distortion in terms of mirror symmetry. Among odd-membered unsubstituted dendralenes, increasing the number of double bonds results in more stable molecules, which is represented by a consistently decreasing trend in reflection symmetry. Theoretically, 1*Z*-, 2-, and 3'-phenyl-[3]dendralenes destabilize the biradicaloid transition structure, indicated by extended lifetime at room temperature. The bisector plane of symmetry correctly predicts that these three mono-substituted [3]dendralenes are less symmetric than the unsubstituted counterpart. In contrast, other substituents at C1 of [3]dendralene, including 1*E*-phenyl, 4-nitrophenyl, 4-methoxyphenyl, methoxycarbonyl, and acetoxymethyl exhibit facile DA dimerization behavior and are predicted to be less symmetric with respect to the σ_v plane than [3]dendralene. As the local symmetry measure utilizes the electronic density, it is sensitive to the resonance effects of π -conjugation and induction from electron withdrawing groups.

B. Chiral microenvironment: A hidden factor behind chiral recognition phenomena

Chirality has been always a central subject in a wide range of chemistry research, i.e., medicinal chemistry, catalysis, and materials science. Although two stereoisomers of a chiral molecule share identical connectivity, they interact completely differently with other chiral environments, such as catalysts, enzymes, receptors, or polarized light, resulting in complex chemical behavior. This subtle asymmetry recognition governs many chemical phenomena, from enantioselective synthesis to therapeutic and toxic effects of drugs. Moreover, the spontaneous induction, amplification, and transfer of chirality provide deep insights into reaction mechanisms, stereoselectivity, and even the origin of biological homochirality.

Local symmetry directly connects to the concept of local chirality. By definition, chiral molecules lack second-order symmetry elements (improper rotations), typically a reflection

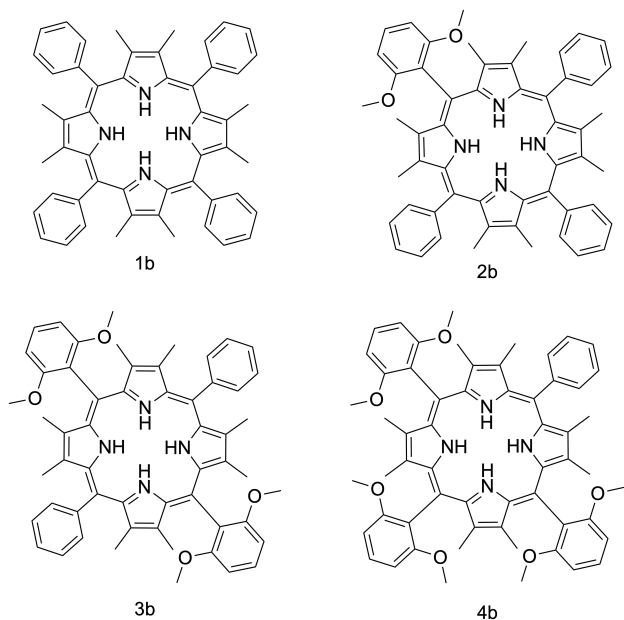


FIG. 4. Tetraphenyl-octamethylporphyrin and dimethoxyphenyl-substituted derivatives. The diprotonated structures are depicted in accordance with the carboxylic acid-complexed crystal structure.

plane or inversion center. Consequently, chirality is an intrinsic property of a molecule whose non-superposable mirror images form distinct enantiomers. On the other hand, a molecule is categorized as achiral if it is superposable on its reflection (or inversion). By quantifying the degree of local symmetry, we can quantify chirality, discretized in a constrained region, which we term the chiral microenvironment. In this section, we present how local chiral microenvironment manifests the chiral recognition phenomena of substituted (5,10,15,20)-tetraphenyl-octamethylporphyrins.

Porphyrins have been extensively studied for many decades from pure chemistry and biology to applied studies in the fields of pharmaceutical science, materials, devices, and many others. In chemical aspect, porphyrin structures possess a macrocyclic skeleton consisting of four pyrrole rings bridged by *meso* methines in 1,3-positions, forming one of the most highly symmetrical molecular shapes in macromolecular chemistry. The most interesting feature of porphyrins is their flexibility to acquire distinctive chemical behavior through engineered functionalization. Obviously, there are 12 available positions on the porphyrin core that can be modified: 4 *meso* positions on the bridges and 8 β positions on the pyrrole units. While β substitutions are widely considered to be the most powerful approach to

alter a porphyrin’s properties and reactivity, *meso* phenyl substitutions have been shown to disrupt the overall planarity of the system, breaking the nominal D_{4h} symmetry, and even producing chiral derivatives.^{40–42} In this manuscript, we focus on a class of porphyrins with methyl groups in all β positions, and either phenyl or 2,6-dimethoxyphenyl substitutions in *meso* positions (Figure 4). **1b** is the “base” tetraphenylporphyrin, whereas **2b–4b** successively substitute dimethoxyphenyl groups, producing a range of global symmetries and, as discussed below, local chiral environments. As **1b** exhibits the highest D_{2d} symmetry, it is achiral. In contrast, **2b** and **4b** possess a single C_2 rotation, while **3b** presents D_2 symmetry with three rotation axes. All substituted porphyrins are therefore chiral. Due to their partial symmetry, the two sides of the molecular plane of all systems behave identically.

These particular porphyrins are reported as effective hosts for sensing asymmetric carboxylic acids, e.g. (R)- and (S)-mandelic acid. In particular, **3b** has the highest chiral selection efficiency with mandelate.⁴⁰ **1b** has no preference between the two enantiomers due to its high symmetry. Yamaguchi et al. resolved the x-ray crystal structure of the mandelate complex of **3b** and showed that the porphyrin adopts a saddle conformation, in which adjacent pyrrole units tilt alternatively.⁴¹ This arrangement reduces the steric repulsion induced by aryl substitutions on the porphyrin periphery, resulting in equivalent up- and down-regions with respect to the quasi-molecular plane. In the complex, **3b** recognizes the chiral guest by two identical hydrogen bonds between N–H bonds from two facing pyrroles and the carboxylate group, as the acidic proton is transferred completely to the porphyrin. More importantly, electrostatic interactions between the mandelate side chain and aryl groups on the porphyrin can play a critical role to favor one enantiomer over the other. Analyzing these nonspecific interactions is challenging, thus, there is no clear explanation towards the chiral recognition strength of the porphyrins. We propose that the unique chiral selection of the porphyrin is enabled by the existence of a local chiral environment generated by dissimilar substitutions on beta-positions.

First, we quantify the local chirality, which is equivalent to chirotopicity concept of Mislow and Siegel,²⁴ at a grid of points around the porphyrins. The fractional lack of reflection or inversion symmetry centered at that point, for a sampling of the electronic density in the local region, therefore represents a chiral microenvironment localized at the evaluating point. The grid boxes are centered at the center of mass of the porphyrins, and extend 3 bohr from the edge of the molecule in each dimension to ensure the box sufficiently covers the molecular

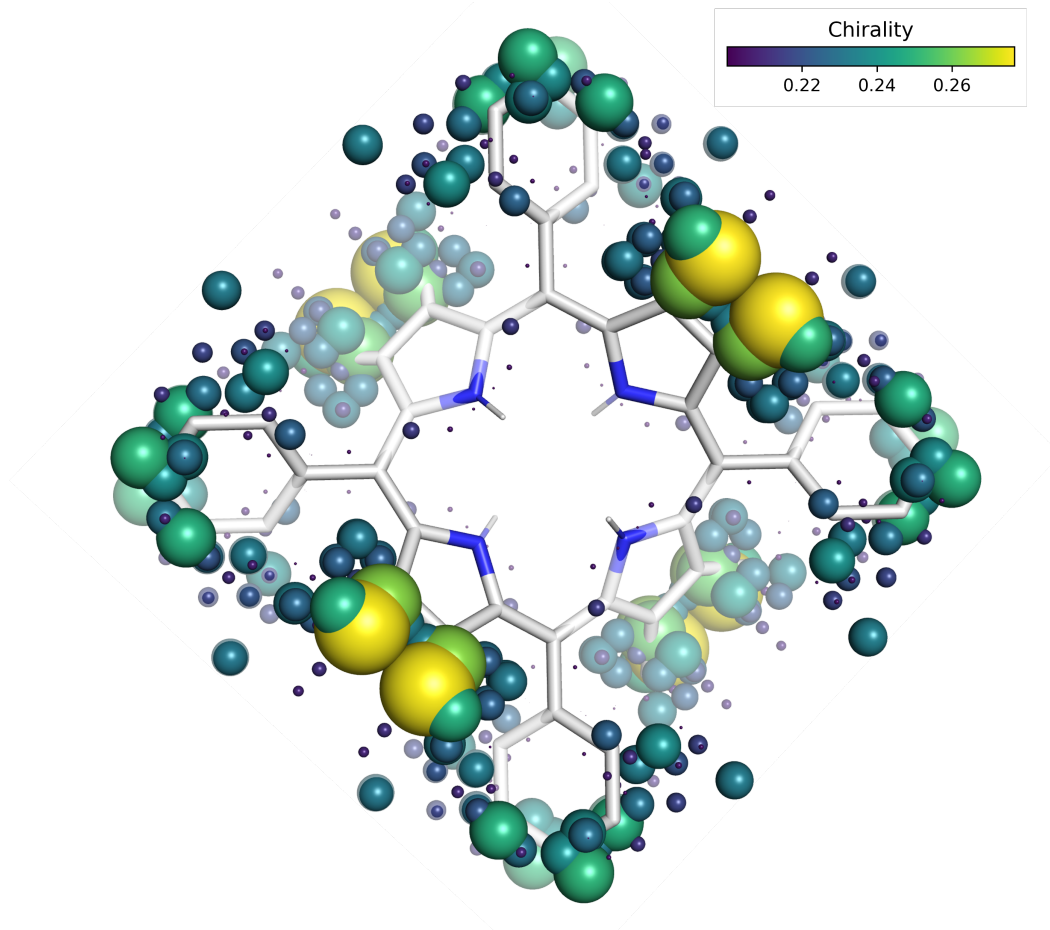


FIG. 5. Chirotopicity field in unsubstituted porphyrin (**1b**)

environment. Computational grids are uniform distributed and include 30 points along each direction. Since the grid points are dense and the coverage of radical functions is greater than the resolution of the grid, the radius of sampling basis functions plays a lesser role. Although only **1b** is achiral compared to the other chiral counterparts, the mean values of its chirotopicity field are consistently higher than for **2b–4b**.

Figures 5 and 6 illustrate the spatial distribution of the chirality field in porphyrins. For the sake of visualization, we exclude points that have chirality lower than 0.2. High chirality is predominantly localized on peripheral substituents, while inner porphyrin core remains largely achiral due to minimal electronic contributions from meso-substituents. The overall chiral patterns reflect the symmetry of the parent structure. In **1b**, the highest chirality are found around beta-methyl moieties on pyrroles, indicating a complex distortion involving the nitrogen atom and adjacent phenyl rings. The four beta-phenyl groups present

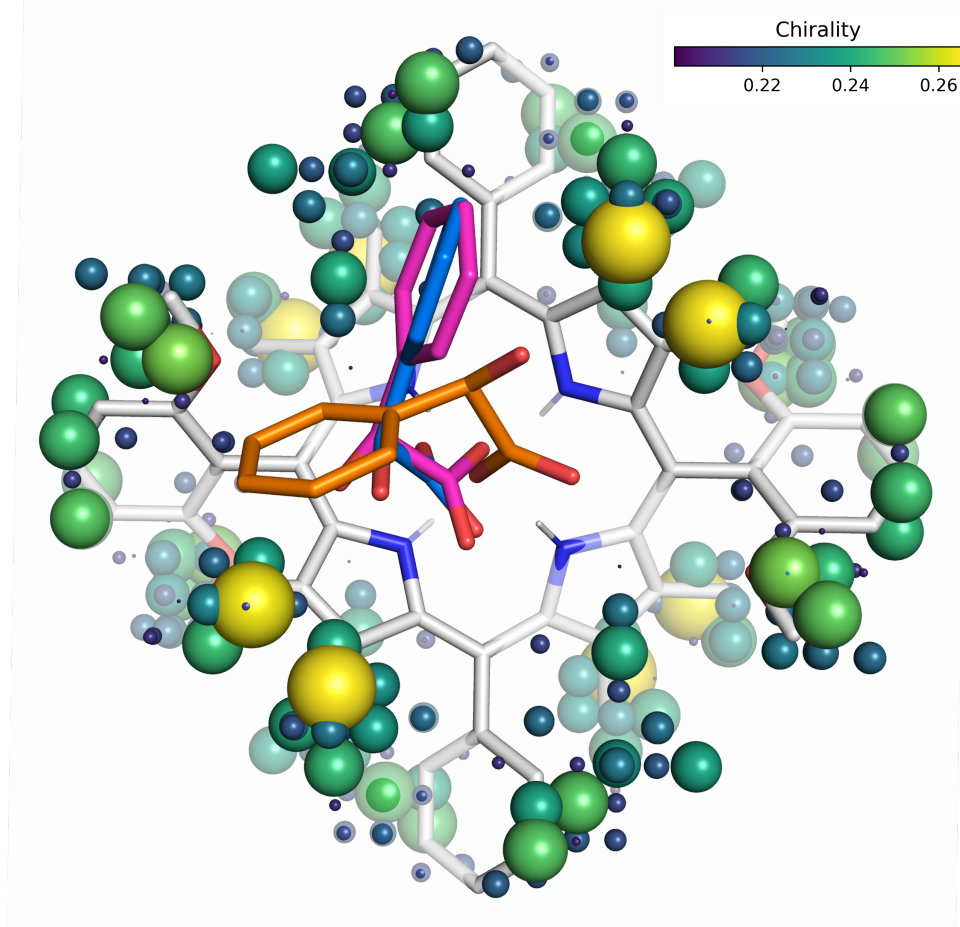


FIG. 6. Chirotopicity field in disubstituted porphyrin (**3b**) with co-crystallized (*S*)-mandelic (blue), modeled (*S*)-mandelic acid (purple), and modeled (*R*)-mandelic acid (orange)

equivalent chiral degree underlying the molecular plane. Substituting a meso-phenyl with a dimethoxyphenyl group in **2b** shifts the maximum chirality to the new substituent and neighboring phenyls. However, the richer chirality on the two phenyl ring surprisingly points outward the dimethoxyphenyl group, conserving the C_2 symmetry. The remaining phenyl shows reduced chirality, indicating a chirality transfer from C15 to C10 and C20 positions on the porphyrin core. With higher total symmetry, excessive chirality regions in **3b** reverts to the pyrrole which is similar to what observed in **1b**, suggesting that the molecular symmetry constrains the meso-substituents, producing a more uniform chiral field. In **4b**, the highest chirality is associated with the dimethoxyphenyl along the in-plane C_2 axis, but also localizes between the other two dimethoxyphenyl groups and on top of the pyrrole rings. More importantly, there are high chirality corridors confined between an *o*-dimethoxyphenyl,

tilted-down pyrrole, and the phenyl groups, exhibited in chiral porphyrins **2b–4b**, but lack in achiral molecule **1b**. Due to the excessive symmetry level, **3b** exhibits four hostpots above each pyrrole, whereas **2b** and **4b** possess two such regions. This chirality signature region is confirmed as recognition site between **3b** and mandelic acid guest. Moreover, the dominant number of chirality corridors on **3b** over **2b** and **4b** also justifies the greatest chirality-transfer efficiency of **3b** among the chiral porphyrins.

Finally, we analyzed the interactions of (S)- and (R)-mandelic acid with chiral porphyrins **2b–4b** using B3LYP/6-31G(d) with D3 dispersion and SMD solvation in 1,2-dichloroethane.³⁹ The porphyrin configurations used in this manuscript are favorable for (S)-mandelate, and inverting the arrangement would favor the (R)-enantiomer. As shown in Figure 6, (S)-mandelate is stabilized above the recognition site of the porphyrins. On the other hand, unfavorable (R)-configuration is oriented away from the recognition region, instead pointed toward the titled-up pyrrole. This binding mode increases the steric repulsion and destabilizes the complex. The crystallographic complex of **3b** with (S)-mandelic acid was used to evaluate the accuracy of the computational models. Alignment of the modeled (S)-mandelic acid with the experimental pose yields a RMSD of 1.170 Å. These findings demonstrate that the porphyrins’ chirality signature, which distinguishes **2b–4b** from **1b**, functions as a selective recognition factor for chiral guest molecules.

IV. CONCLUSION

Although symmetry underlies a wide range of chemical concepts, current symmetry-driven theories have remained largely qualitative in explaining experimental phenomena. In this study, we introduce an algorithm that connects hidden local symmetry features with a continuous scale, enabling quantitative correlations with molecular properties. Using local diene motifs in dendralenes as a case study, we demonstrated how their intrinsic symmetry governs molecular properties such as stability, Diels–Alder reactivity, and distinctive spectroscopic signatures. Furthermore, we presented a chirality field to quantify microscopic chirality embedded within a molecular framework. Notably, the chiral environment mapped for porphyrins reveals a distinct region that critically enables their enhanced chiral recognition toward chiral carboxylic acids.

Since the method captures both discrete and continuous considerations of symmetry at

a fine-grained spatial resolution, it offers significant potential for broader applications. For example, one can apply the method to analyze dynamic symmetry breaking in reaction pathways, quantify conformational deformation and aggregation, and reveal non-specific interactions in complex molecular assemblies. Its generality also makes it suitable for studying symmetry-driven behavior in supramolecular systems, catalytic cavities, and bimolecular environments, where traditional symmetry descriptors exhibit limitations. The approach also opens new areas for systematically linking local symmetry metrics to structure-property relationships across various classes of chemical systems.

ACKNOWLEDGEMENTS

This work was supported in part by the US National Science Foundation (grant CHE-2143725) and by the US Department of Energy (grant DE-SC0022893). Computational resources for this research were provided by SMU’s O’Donnell Data Science and Research Computing Institute.

CONFLICT OF INTEREST STATEMENT

The authors declare no competing conflicts of interest.

REFERENCES

- ¹R. B. Woodward and R. Hoffmann, “The Conservation of Orbital Symmetry,” *Angewandte Chemie International Edition in English* **8**, 781–853 (1969), eprint: <https://onlinelibrary.wiley.com/doi/pdf/10.1002/anie.196907811>.
- ²R. G. Pearson, “Symmetry rules for chemical reactions,” *Computers & Mathematics with Applications* **12**, 229–236 (1986).
- ³G. L. Caldow and R. A. MacGregor, “Some symmetry aspects of homogeneous catalysis,” *Inorganic and Nuclear Chemistry Letters* **6**, 645–649 (1970).
- ⁴Z. B. Maksić, “Symmetry, hybridization and bonding in molecules,” *Computers & Mathematics with Applications* **12**, 697–723 (1986).
- ⁵R. Hoffmann, “Interaction of orbitals through space and through bonds,” *Accounts of Chemical Research* **4**, 1–9 (1971), publisher: American Chemical Society.

- ⁶D. J. Cram and J. M. Cram, “Host-Guest Chemistry,” *Science* **183**, 803–809 (1974), publisher: American Association for the Advancement of Science.
- ⁷Y. Sang, M. Liu, Y. Sang, and M. Liu, “Symmetry Breaking in Self-Assembled Nanoassemblies,” *Symmetry* **11** (2019), 10.3390/sym11080950, company: Multidisciplinary Digital Publishing Institute Distributor: Multidisciplinary Digital Publishing Institute Institution: Multidisciplinary Digital Publishing Institute Label: Multidisciplinary Digital Publishing Institute Publisher: publisher.
- ⁸Y. Sang and M. Liu, “Hierarchical self-assembly into chiral nanostructures,” *Chemical Science* **13**, 633–656 (2022), publisher: Royal Society of Chemistry.
- ⁹I. B. Bersuker, “The Jahn-Teller and pseudo Jahn-Teller effect in materials science,” *Journal of Physics: Conference Series* **833**, 012001 (2017), publisher: IOP Publishing.
- ¹⁰I. B. Bersuker, “Jahn–Teller and Pseudo-Jahn–Teller Effects: From Particular Features to General Tools in Exploring Molecular and Solid State Properties,” *Chemical Reviews* **121**, 1463–1512 (2021), publisher: American Chemical Society.
- ¹¹P.-P. Shi, Y.-Y. Tang, P.-F. Li, W.-Q. Liao, Z.-X. Wang, Q. Ye, and R.-G. Xiong, “Symmetry breaking in molecular ferroelectrics,” *Chemical Society Reviews* **45**, 3811–3827 (2016), publisher: The Royal Society of Chemistry.
- ¹²J. M. Duarte, S. Dutta, D. S. Goodsell, and S. K. Burley, “Exploring protein symmetry at the RCSB Protein Data Bank,” *Emerging Topics in Life Sciences* **6**, 231–243 (2022).
- ¹³S. Keinan and D. Avnir, “Quantitative Symmetry in Structure–Activity Correlations: The Near C₂ Symmetry of Inhibitor/HIV Protease Complexes,” *Journal of the American Chemical Society* **122**, 4378–4384 (2000), publisher: American Chemical Society.
- ¹⁴M. Petitjean, “Chirality and Symmetry Measures: A Transdisciplinary Review,” *Entropy* **5**, 271–312 (2003), company: Molecular Diversity Preservation International Distributor: Molecular Diversity Preservation International Institution: Molecular Diversity Preservation International Label: Molecular Diversity Preservation International Publisher: publisher.
- ¹⁵H. Zabrodsky, S. Peleg, and D. Avnir, “Continuous symmetry measures,” *Journal of the American Chemical Society* **114**, 7843–7851 (1992), publisher: American Chemical Society.
- ¹⁶P. G. Mezey, “The degree of similarity of three-dimensional bodies: Application to molecular shape analysis,” *Journal of Mathematical Chemistry* **7**, 39–49 (1991).

- ¹⁷A. Ferrarini and P. L. Nordio, "On the assessment of molecular chirality," *Journal of the Chemical Society, Perkin Transactions 2* , 455–460 (1998), publisher: The Royal Society of Chemistry.
- ¹⁸S. Grimme, "Continuous symmetry measures for electronic wavefunctions," *Chemical Physics Letters* **297**, 15–22 (1998).
- ¹⁹J. J. Aucar, A. Stroppa, and G. A. Aucar, "A Relationship between the Molecular Parity-Violation Energy and the Electronic Chirality Measure," *The Journal of Physical Chemistry Letters* **15**, 234–240 (2024), publisher: American Chemical Society.
- ²⁰S. Shah, V. S. R. Ganga, Y.-X. Huang, N. Fridman, I. Tuvi-Arad, Y.-T. Chan, O. Reany, and E. Keinan, "Calochorturils: Chiral Bowl-Shaped Cavitands Obtained by Anisotropic Tangential Substitution," *Journal of the American Chemical Society* **147**, 38443–38451 (2025), publisher: American Chemical Society.
- ²¹C. Guo, C. Putzke, S. Konyzheva, X. Huang, M. Gutierrez-Amigo, I. Errea, D. Chen, M. G. Vergniory, C. Felser, M. H. Fischer, T. Neupert, and P. J. W. Moll, "Switchable chiral transport in charge-ordered kagome metal CsV3Sb5," *Nature* **611**, 461–466 (2022), publisher: Nature Publishing Group.
- ²²P. W. Fowler, "Vocabulary for fuzzy symmetry," *Nature* **360**, 626–626 (1992), publisher: Nature Publishing Group.
- ²³A. Grieder, S. Tu, and Y. Ping, "Relation of Continuous Chirality Measure to Spin and Orbital Polarization, and Chiroptical Properties in Solids," *Advanced Optical Materials* **13**, e01190 (2025), eprint: <https://advanced.onlinelibrary.wiley.com/doi/pdf/10.1002/adom.202501190>.
- ²⁴K. Mislow and J. Siegel, "Stereoisomerism and local chirality," *Journal of the American Chemical Society* **106**, 3319–3328 (1984), publisher: American Chemical Society.
- ²⁵P. F. J. Lipiński and J. C. Dobrowolski, "Local chirality measures in QSPR : IR and VCD spectroscopy," *RSC Advances* **4**, 47047–47055 (2014), publisher: The Royal Society of Chemistry.
- ²⁶S. Alvarez, P. Alemany, and D. Avnir, "Continuous chirality measures in transition metal chemistry," *Chemical Society Reviews* **34**, 313–326 (2005), publisher: The Royal Society of Chemistry.
- ²⁷Q. Sun, T. C. Berkelbach, N. S. Blunt, G. H. Booth, S. Guo, Z. Li, J. Liu, J. D. McClain, E. R. Sayfutyarova, S. Sharma, S. Wouters, and G. K.-L. Chan, "PySCF: the Python-

- based simulations of chemistry framework,” *WIREs Computational Molecular Science* **8**, e1340 (2018), [_eprint: https://wires.onlinelibrary.wiley.com/doi/pdf/10.1002/wcms.1340](https://wires.onlinelibrary.wiley.com/doi/pdf/10.1002/wcms.1340).
- ²⁸Q. Sun, X. Zhang, S. Banerjee, P. Bao, M. Barbry, N. S. Blunt, N. A. Bogdanov, G. H. Booth, J. Chen, Z.-H. Cui, J. J. Eriksen, Y. Gao, S. Guo, J. Hermann, M. R. Hermes, K. Koh, P. Koval, S. Lehtola, Z. Li, J. Liu, N. Mardirossian, J. D. McClain, M. Motta, B. Mussard, H. Q. Pham, A. Pulkin, W. Purwanto, P. J. Robinson, E. Ronca, E. R. Sayfutyarova, M. Scheurer, H. F. Schurkus, J. E. T. Smith, C. Sun, S.-N. Sun, S. Upadhyay, L. K. Wagner, X. Wang, A. White, J. D. Whitfield, M. J. Williamson, S. Wouters, J. Yang, J. M. Yu, T. Zhu, T. C. Berkelbach, S. Sharma, A. Y. Sokolov, and G. K.-L. Chan, “Recent developments in the PySCF program package,” *The Journal of Chemical Physics* **153**, 024109 (2020).
- ²⁹F. Neese, “Software Update: The ORCA Program System—Version 6.0,” *WIREs Computational Molecular Science* **15**, e70019 (2025), [_eprint: https://wires.onlinelibrary.wiley.com/doi/pdf/10.1002/wcms.70019](https://wires.onlinelibrary.wiley.com/doi/pdf/10.1002/wcms.70019).
- ³⁰E. G. Mackay and M. S. Sherburn, “Demystifying the dendralenes,” *Pure and Applied Chemistry* **85**, 1227–1239 (2013), publisher: De Gruyter.
- ³¹H. Hopf, “The Dendralenes—a Neglected Group of Highly Unsaturated Hydrocarbons,” *Angewandte Chemie International Edition in English* **23**, 948–960 (1984), [_eprint: https://onlinelibrary.wiley.com/doi/pdf/10.1002/anie.198409481](https://onlinelibrary.wiley.com/doi/pdf/10.1002/anie.198409481).
- ³²S. Woo, N. Squires, and A. G. Fallis, “Indium-Mediated γ -Pentadienylation of Aldehydes and Ketones: Cross-Conjugated Trienes for Diene-Transmissive Cycloadditions,” *Organic Letters* **1**, 573–576 (1999), publisher: American Chemical Society.
- ³³S. Fielder, D. D. Rowan, and M. S. Sherburn, “First Synthesis of the Dendralene Family of Fundamental Hydrocarbons,” *Angewandte Chemie International Edition* **39**, 4331–4333 (2000), [_eprint: https://onlinelibrary.wiley.com/doi/pdf/10.1002/1521-3773%2820001201%2939%3A23%3C4331%3A%3AAID-ANIE4331%3E3.0.CO%3B2-3](https://onlinelibrary.wiley.com/doi/pdf/10.1002/1521-3773%2820001201%2939%3A23%3C4331%3A%3AAID-ANIE4331%3E3.0.CO%3B2-3).
- ³⁴J. George, J. S. Ward, and M. S. Sherburn, “A general synthesis of dendralenes,” *Chemical Science* **10**, 9969–9973 (2019), publisher: The Royal Society of Chemistry.
- ³⁵M. F. Saglam, T. Fallon, M. N. Paddon-Row, and M. S. Sherburn, “Discovery and Computational Rationalization of Diminishing Alternation in [n]Dendralenes,” *Journal of the American Chemical Society* **138**, 1022–1032 (2016), publisher: American Chemical Society.

- ³⁶M. F. Saglam, A. R. Alborzi, A. D. Payne, A. C. Willis, M. N. Paddon-Row, and M. S. Sherburn, "Synthesis and Diels–Alder Reactivity of Substituted [4]Dendralenes," *The Journal of Organic Chemistry* **81**, 1461–1475 (2016), publisher: American Chemical Society.
- ³⁷S. V. Pronin and R. A. Shenvi, "Synthesis of a Potent Antimalarial Amphilectene," *Journal of the American Chemical Society* **134**, 19604–19606 (2012), publisher: American Chemical Society.
- ³⁸A. D. Payne, G. Bojase, M. N. Paddon-Row, and M. S. Sherburn, "Practical Synthesis of the Dendralene Family Reveals Alternation in Behavior," *Angewandte Chemie International Edition* **48**, 4836–4839 (2009), eprint: <https://onlinelibrary.wiley.com/doi/pdf/10.1002/anie.200901733>.
- ³⁹A. V. Marenich, C. J. Cramer, and D. G. Truhlar, "Universal Solvation Model Based on Solute Electron Density and on a Continuum Model of the Solvent Defined by the Bulk Dielectric Constant and Atomic Surface Tensions," *The Journal of Physical Chemistry B* **113**, 6378–6396 (2009), publisher: American Chemical Society.
- ⁴⁰Y. Furusho, T. Kimura, Y. Mizuno, and T. Aida, "Chirality-Memory Molecule: A D₂-Symmetric Fully Substituted Porphyrin as a Conceptually New Chirality Sensor," *Journal of the American Chemical Society* **119**, 5267–5268 (1997), publisher: American Chemical Society.
- ⁴¹Y. Mizuno, T. Aida, and K. Yamaguchi, "Chirality-Memory Molecule: Crystallographic and Spectroscopic Studies on Dynamic Molecular Recognition Events by Fully Substituted Chiral Porphyrins," *Journal of the American Chemical Society* **122**, 5278–5285 (2000), publisher: American Chemical Society.
- ⁴²S. A. Syrbu, T. V. Lyubimova, and A. S. Semeikin, "Phenyl-substituted porphyrins. 1. Synthesis of meso-phenyl-substituted porphyrins," *Chem Heterocycl Compd* **40**, 1262–1270 (2004).